

A far-infrared heterodyne sidebands spectrometer

D. Boucher, R. Bocquet, J. Burie, W. M. Chen

▶ **To cite this version:**

D. Boucher, R. Bocquet, J. Burie, W. M. Chen. A far-infrared heterodyne sidebands spectrometer. Journal de Physique III, 1994, 4 (8), pp.1467-1480. 10.1051/jp3:1994214 . jpa-00249197

HAL Id: jpa-00249197
https://hal.science/jpa-00249197

Submitted on 4 Feb 2008

HAL is a multi-disciplinary open access archive for the deposit and dissemination of scientific research documents, whether they are published or not. The documents may come from teaching and research institutions in France or abroad, or from public or private research centers.

L'archive ouverte pluridisciplinaire **HAL**, est destinée au dépôt et à la diffusion de documents scientifiques de niveau recherche, publiés ou non, émanant des établissements d'enseignement et de recherche français ou étrangers, des laboratoires publics ou privés.

Classification
Physics Abstracts
07.62 — 07.65 — 42.60B

A far-infrared heterodyne sidebands spectrometer

D. Boucher ([1]), R. Bocquet ([1]), J. Burie ([2]) and W. Chen ([2])

([1]) Laboratoire de Spectroscopie Hertzienne, URA 249 CNRS, Université des Sciences et Technologies de Lille, 59650 Villeneuve d'Ascq, France
([2]) Laboratoire de Physico-Chimie de l'Atmosphère, Université du Littoral, Quai Freycinet, 59375 Dunkerque, France

(*Received 9 March 1994, accepted 17 May 1994*)

Abstract. — We present recent experimental developments in far-infrared coherent spectroscopy. Most known far-infrared sidebands spectrometers use the direct detection scheme. The system developed at Lille operates in the heterodyne mode. This technique offers particular advantages when large detection instantaneous bandwidths are needed, as could be the case in time resolved spectroscopy. As a counterpart of a heavier electronic receiver system, the filtering constraints in the optical path are totally eliminated, leading to a potential lowering of the overall noise system. The receiver operates very close to physical limits. A carefully designed optical line, incorporating only reflective components, allows to keep optical losses at very low levels, on the whole operating range. By using particular laser injection coupling and power extraction schemes, reasonable short and long term stability has been achieved in sidebands power generation. Some spectroscopic results illustrating sensitivity and resolution capabilities are presented.

1. Introduction.

For many purposes in high resolution spectroscopy it is desirable to have a coherent, continuously tunable radiation source. Due to a lack of readily available such sources, experimental work at frequencies between 300 and 3 000 GHz suffers severe limitations. Most investigations in the field are done by the Fourier transform technique. At long wavelengths, the major limitation in sensitivity of Fourier transform spectrometers results from the very weak blackbody brightness. It should be possible to increase performances by using the synchrotron radiation as light source. In this case, very large accelerator systems are needed. This solution is restricted to some large national or international facilities. On the other hand, expected sensitivities will remain some order of magnitude worse than achieved in the neighbouring millimeter or infrared ranges where monochromatic, coherent and frequency tunable light sources exist at reasonable power levels.

With the apparition of optically pumped molecular lasers, emitting on a rapidly growing number of emissions lines with powers in excess of some tens of milliwatts, the sidebands generation principle became very attractive.

Schematically, this principle consists of mixing a far-infrared fixed frequency ν_L laser emission with a tunable frequency $\Delta\nu$, in order to produce :

$$\nu = \nu_L \pm n \, . \, \Delta\nu \, . \tag{1}$$

Some radiation generators operate using this principle in the far-infrared range. The instruments developed at Berkeley [1], Caltech [2], Nijmegen [3] and at Lille [4] were probably pioneers in the field.

The three first mentioned systems rely on a similar principle. They retain a $\Delta\nu$ frequency in the millimeter range and a direct detection scheme. The system developed at Lille is of a radically different design. The $\Delta\nu$ frequency is chosen in the centimeter range and the receiver system is heterodyne. A similar instrument was developed some years ago by Fetterman *et al.* [5, 6].

In our present work, we shall describe the essential features of the heterodyne spectrometer. The heterodyne principle has some particular advantages compared to the direct detection one and in particular very broad instantaneous bandwidth capabilities. Observations of very fast transient phenomena are possible, for instance in pulsed supersonic molecular beams.

The lack of tunable local oscillators constitutes the major obstacle to the development of heterodyne systems in the far-infrared range. This difficulty has been overcome using two successive down conversions. The tunability requirements are translated in the centimeter range where high performance solutions are more easily found.

2. The sidebands generation principle.

The frequency mixing is performed in non linear Schottky diode systems and is similar for all known instruments. These mixers will be described in part 3.2. The mixing process efficiency is low. At the throughput of the mixer, the optical beam contains a very strong component at the fundamental frequency ν_L and sidebands components at $\nu_L \pm \Delta\nu$. The order of magnitude of the power ratio $\dfrac{P(\nu_L)}{P(\nu_L \pm \Delta\nu)}$ is currently of 10^3 or more.

All frequency components are radiated in a spatially unique optical beam.

The basic operating mode of a direct detection apparatus is shown at figure 1.

For all known direct detection spectrometers, the detectors are cryogenic systems with very low power saturation thresholds. An efficient rejection filter at ν_L is then always needed. Nijmeguen and Berkeley systems depart mainly in the design of this filtering system.

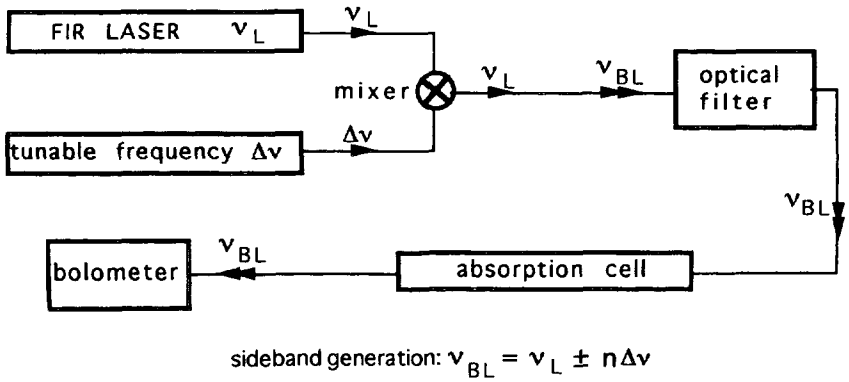


Fig. 1. — The baseband detection scheme.

The former uses a grating dispersive device.

The later incorporates a Martin-Pupplett polarising interferometer, previously described in several papers [7, 8].

In both cases the fundamental laser radiation suppression remains very incomplete. This parasitic power exceeds noticeably the useful sidebands power at the detector entrance. This remark remains true even when using the best filtering systems.

In order to improve the filtering process, direct detection spectrometers usually retain the higher $\Delta\nu$ compatible with the mixer technology, falling in the millimeter range.

When the capabilities of this high performance systems are carefully analysed, it is found that the parasitic radiation level establishes the sensitivity limit.

The spectrometer developed at Lille has a different design as shown at figure 2.

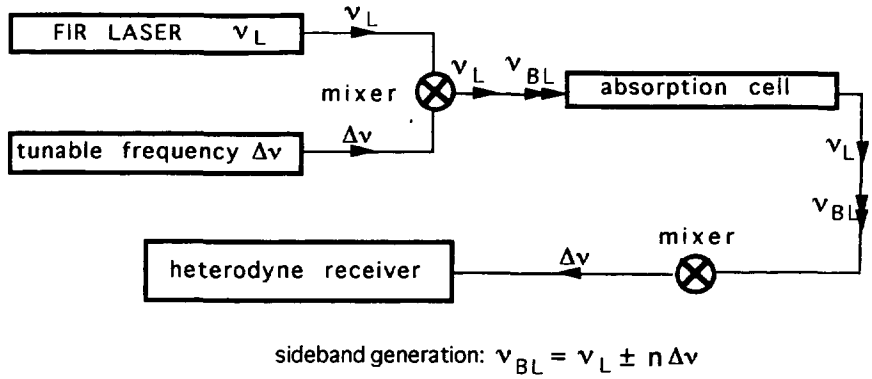


Fig. 2. — The heterodyne detection scheme.

After the mixing process, the whole optical power is transmitted through the spectroscopic sample before reaching a far-infrared mixer. The mixing process provides a beat note at $\Delta\nu$ containing the potential experimental information. Not any optical separation is needed, and so, low values for the $\Delta\nu$ frequency are allowed. In the actual version of the system $\Delta\nu$, has been chosen between 2 and 20 GHz. Very low noise amplifiers and receiver components are available in this frequency domain.

The beat note is processed using purely electronic means, according to usual heterodyne methods.

An apparent drawback of this technique lies in the simultaneous irradiation of the sample by both local oscillator and sidebands radiations. Some tens of molecular species have been investigated using this instrument without observing any trouble. Such trouble could only occur in case of accidental coincidence between transitions at ν_L and $\nu_L \pm \Delta\nu$.

3. Description of the spectrometer.

Figure 3 gives a schematic view of the spectrometer. On the basis of the previous description the instrument can be divided in functional blocks. The original parts of these blocks will be described in detail below.

This blocks are : the laser system, the optical system including the sidebands generator, the heterodyne receiver and the data processing system.

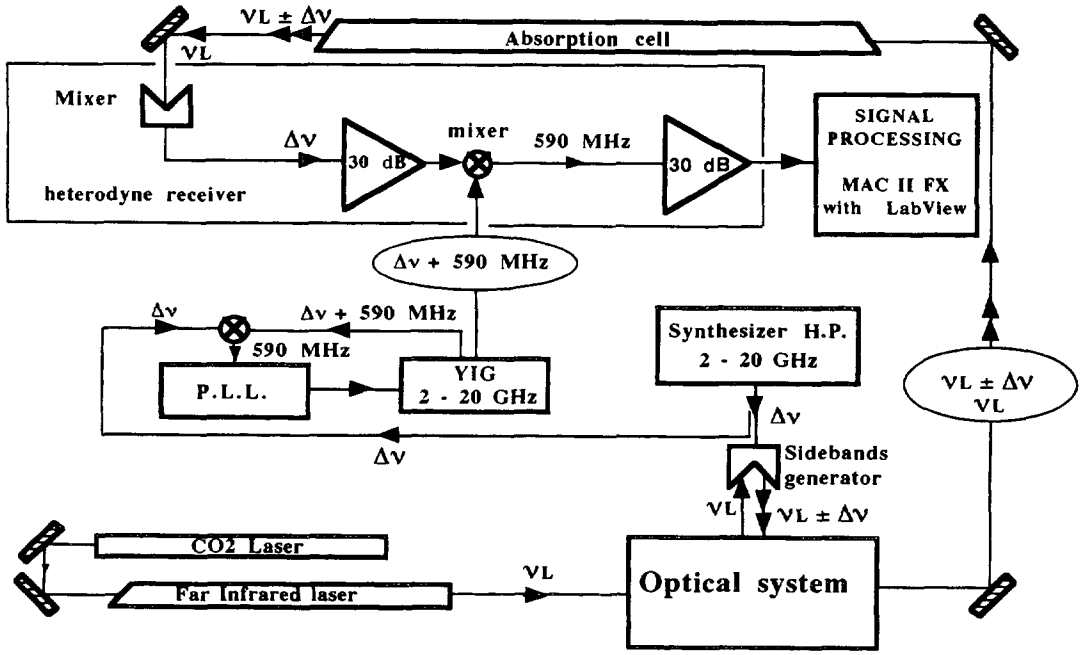


Fig. 3. — The tunable Far Infrared spectrometer.

3.1 THE LASER SYSTEM. — The fundamental far-infrared radiation is emitted by an optically pumped molecular laser. This laser has been designed in the main attempts of very high stabilities for both frequency and power. A power in excess of 10 mW on at least some tens of emissions, regularly distributed between 500 and 3 000 GHz was expected.

The carbon dioxide pump laser is a commercial device. It is a PL6 model manufactured by Edimburgh Instruments. It delivers a peak power of the order of 180 W on strongest emissions and oscillates on about 100 lines. This power remains of the order of 30 W on lines such as 9R4 or 10R46.

The far-infrared laser is a lab made instrument. It is of a waveguided type. The waveguide consists of a 3 meter long, free of scratch, 38 mm bore straight section of quartz pipe.

At the laser input, the pump power is injected through a 2 mm bore alumina waveguide. The pump beam is focused to a spot diameter 0.6 times smaller than the waveguide diameter [9, 10]. Resulting from natural diffraction effects, the emerging beam waist diameter is approximately 19 mm after a 3 meters path, corresponding to half the laser cavity diameter. This situation corresponds to the well-known optimal filling factor condition [11].

The far-infrared laser is water-cooled. The power is extracted *via* a gold plated silicon coupler. The flat output mirror is covered with a 10 microns thick gold layer excepted at the center where a 8 mm central window remains uncoated. The device insures the output coupling and the laser vacuum integrity.

The main difficulty encountered in the development of the spectrometer has been the unstable behavior of the laser system. The power retroreflection to the pump laser has been recognized as the essential cause of instabilities. Using the previously described techniques, a sufficiently low pump power retroreflection rate has been reached and so, the main origin of laser instabilities has been largely minimised. An other important characteristic stands in the good compatibility of involved technologies with high pump powers. For instance, a very

efficient output coupling method using lithographic grids on quartz substrates has been forsaken. Couplers were rapidly destroyed under the high pump beam illumination.

The laser emission is servo-controlled. A miniaturised electret microphone is located inside the far-infrared laser. The CO_2 laser cavity length is modulated using a piezo-electric translator, leading to a frequency modulation of the laser emission. The modulation frequency is 220 Hz. The sweep modulation depth of the pump frequency is usually in order of 100 kHz.

The lasing transition in the far-infrared active laser media acts as a frequency discriminator. The amplitude of the acoustic signal measures the pump frequency detuning. Its phase indicates the sign of that detuning. So, after filtering and phase detection of the acoustic response, the resulting information is used as correction signal for the frequency control of the CO_2 laser. It is connected to the control input of the commercial piezo-electric translator driver, and so, adjusts the cavity length.

Natural fluctuations are negligible beyond 30 Hz. The stabilization loop efficiently corrects slow fluctuations of thermal origin. After a 1 hour thermalization lap, the laser system reaches a very stable regime, allowing several hours long working sessions. Table I summarizes the set of molecular emissions used in the present experiment. The frequency measurements of CH_2CHF emissions at 634 GHz, 673 GHz, 889 GHz and 902 GHz had not been previously reported.

Taking into account a sweeping capability of 36 GHz for each laser emission (using only $n = 1$ in formula (1)) the spectral coverage is about 60 % on the wavelength range 500-1 500 GHz and about 30 % between 1 500 and 2 500 GHz. This spectral coverage could be noticeably expanded by further systematic investigations of powerful laser lines, in particular on isotopically substituted molecular species.

3.2 OPTICAL AND SIDEBANDS GENERATOR SYSTEMS. — A view of the optical system is given at figure 4. Three distinct functions have to be performed through the optical system :

i) 50 % coupling of the FIR laser power towards the sidebands generator ;

ii) 50 % coupling of the FIR laser power towards the receiver through the absorption cell. Corresponding to the usual heterodyne terminology, this part acts as the local oscillator ;

iii) coupling of the full sidebands power towards the front end receiver mixer through the absorption cell.

In a first version of the spectrometer, the i, ii, iii previously described functions had been performed using a rustic device. This system consisted of a mylar beam splitter and a plane reflector. Although replaced by a more sophisticated set-up, the preliminary version is well-suited for a description of the basic working principle of the optical part. A schematic view of this simplified system is given at figure 5.

Such a device has some inherently attached drawbacks, and, in particular :

i) resulting from interference effects in the dielectric sheet, the coupling efficiency is strongly dependent on frequency ;

ii) a noticeable power retroreflection rate leading to laser instabilities ;

iii) a 50 % loss in sidebands power resulting from previous remark.

In the most recent version, a new optical system has been built around two Martin-Puppett polarising interferometers [7]. All beam separations and recombinations are performed on metal meshes consisting of one-dimensional arrays of thin wires [13]. Such systems are polarization selective.

Let us recall that :

• for an incident electromagnetic wave with the electric field parallel to the wires the wave is reflected with negligible transmission ;

Table I. — *Usable FIR laser lines.*

frequency GHz	pump line	power pump W	laser molecule	polarisation
584.3882	9R28	75	HCOOH	⊥
590.5511 (a)	10P38	65	CH_2CHF	//
634.2220 (b)	10P20	100	CH_2CHF	⊥
653.8214	9R38	45	HCOOH	⊥
672.3318	9R20	65	HCOOH	
673.9974 (b)	10R20	130	CH_2CHF	⊥
692.9514	9R20	40	HCOOH	//
693.7884	9R22	40	HCOOH	
716.1568	9R22	40	HCOOH	//
739.3403	9P16	150	HDCO	
759.5433	9P6	45	CH_2F_2	⊥
761.6083	9R18	40	HCOOH	//
783.4860	9P10	80	CH_2F_2	//
889.3414 (b)	10P38	80	CH_2CHF	⊥
902.0004 (b)	10P6	50	CH_2CHF	//
991.7778	9R4	20	HCOOH	⊥
1035.5527	9P4	45	CH_2F_2	//
1042.1504	9R34	45	CH_2F_2	//
1076.8428	10P8	60	D_2CO	
1100.8067	9P10	50	CH_2F_2	//
1101.1594	9R24	130	CH_2DOH	
1145.4301	9P38	45	CH_2F_2	⊥
1160.0718	9P16	150	$H^{13}COOH$	
1193.7273	10R38	45	CH_3OH	⊥
1267.0815	9R6	40	CH_2F_2	//
1397.1186	9R34	45	CH_2F_2	⊥
1509.0402	9P38	100	CH_3OH	⊥
1542.5246	9P8	40	HDCO	//
1546.0834	9R22	45	CH_2F_2	
1626.6026	9R32	45	CH_2F_2	⊥
1838.8393	10R38	45	CH_3OH	//
1891.2742	9P10	60	CH_2F_2	//
2216.2635	9P24	65	CH_2F_2	//
2237.2964	9P22	45	CH_2F_2	⊥
2522.7816	9P36	40	CH_3OH	⊥
2546.4950	9R20	45	CH_2F_2	⊥
3105.9368	9R10	65	CH_3OH	//
4251.6740	9P34	60	CH_3OH	

_ laser frequencies are taken from reference [12]
_ the symbol "(a)" indicates frequencies derived from wavelength measurements reported in ref [12].
_ the symbol "(b)" indicates frequencies measured in the actual work

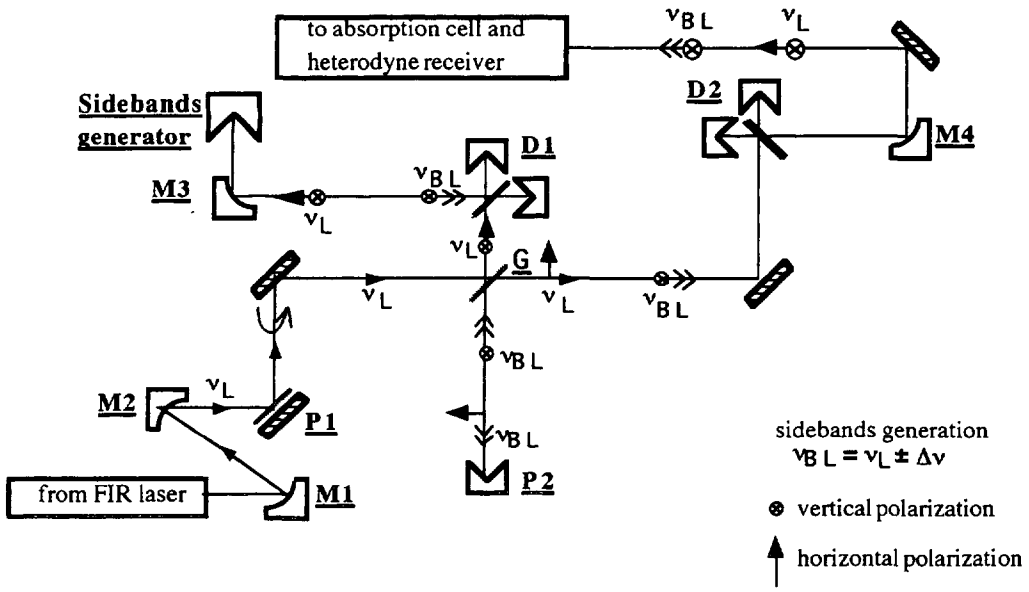


Fig. 4. — The optical system.

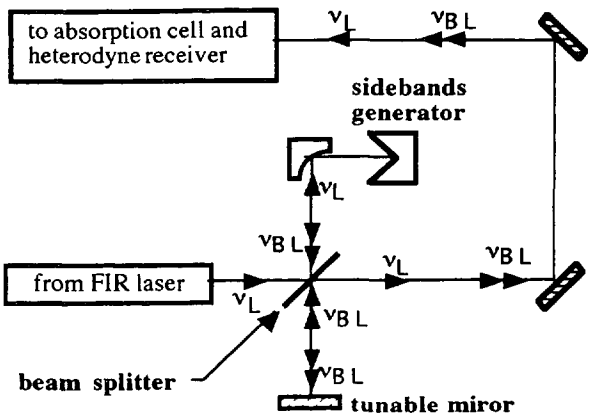


Fig. 5. — A rustic device.

• for an incident electromagnetic wave with the electric field perpendicular to the wires the wave is transmitted with negligible reflection ;

• for a 45° polarized incident beam with a 45° polarization respective to the wires direction, 50 % of the incident power is reflected, 50 % is transmitted.

When properly designed, such devices can easily be made frequency independent on the range 500-3 000 GHz.

For the actual optical set-up, meshes systems have been machined using 10 microns gold plated tungsten wire. The distance between two successive wires is 30 microns.

Schematically, the optical system works as follows : at the laser output, the far-infrared beam is reflected by two successive off axis parabolic mirrors M_1 and M_2 in a telescope arrangement. The mirror focal lengths are respectively 70 and 210 mm. This set-up constitutes a beam expander of 3/1 ratio.

Prior to any power division, the linear polarization of the laser beam is converted to circular polarization by a reflective quarter wave plate P_1, operating at 45° incidence. The quarter wave plate consists of the parallel arrangement of a metal mesh and a plane reflecting mirror. The distance between the metal mesh and the associated reflector is adjustable. By a proper tuning of this distance, any linear polarization state at the input can be converted to the needed one, vertical, elliptic, circular or horizontal, at the output.

A first operation is performed using the vertical grid G with vertical wires. The laser power is divided into two parts :

- 50 % is reflected towards the polarising diplexer D_1, with vertical polarization ;
- 50 % is transmitted towards the polarising diplexer D_2 with horizontal polarization. This part will act as local oscillator for the heterodyne receiver.

The second and more complex operation is performed using the polarising diplexer D_1. The laser beam at ν_L with vertical polarization passes through D_1 and is coupled onto the modulator (sidebands generator) *via* M_3 (50 mm focal length elliptic mirror) with the same polarization state. The sidebands ($\nu = \nu_L \pm n \cdot \Delta\nu$) reemitted by the modulator enter D_1 with vertical polarization and go out with an horizontal polarization state. The D_1 internal pathlength difference is therefore adjusted to obtain :

- a 90° rotation of the sidebands polarization ;
- an unaltered polarization state for the laser beam at ν_L.

The sidebands are then transmitted through the grid G (with vertical wires). They enter a polarization reflector P_2 operating at normal incidence. P_2 consists of a roof top mirror, the apex of which being in a 45° position. Such a system reflects the polarization vector with respect to the line of intersection of its plane surfaces. The incoming horizontally polarized radiation is retroreflected with vertical polarization and so, reflected again by the vertical grid G towards D_2.

The optical beam entering D_2 carries 50 % of the unmodulated power with an horizontal polarization and the whole sidebands power with a vertical polarization.

The last step is achieved by the polarising diplexer D_2. Its pathlength difference is adjusted in order to obtain a vertical polarization, compatible with the mixer antenna direction of the detection diode, for both the sidebands and the local oscillator.

The beam waist is matched to the absorption cell entrance by the 700 mm focus off axis parabolic mirror [10].

The absorption cell consists of a 38 mm bore, 3 m long section of quartz pipe. It is sealed off at both ends using PTFE windows at brewster incidence. This technique allows a limitation of the transmission losses through the absorption cell below 5 % on the range 500-2 500 GHz.

The optical beam is finally matched to the main antenna lobe of the mixer assembly by a 50 mm off axis elliptic mirror.

All optical components are lab made :

- parabolic and elliptic mirrors have been machined using standard milling machines, following the original method described by Erickson [14] and reviewed in our group [15] ;
- the wire grids have been wound on circular frames using a machine inspired by [16] ;
- polarising diplexers D_1 et D_2 are located on a 300 mm by 300 mm base plate in an ultra

compact assembly. The measured rejection rates for the crossed polarization are respectively :

25 dB at 692 GHz
25 dB at 1 100 GHz
16 dB at 1 600 GHz
13 dB at 2 200 GHz
11 dB at 2 500 GHz .

The most important property of this optical part stands in the very low transmission loss achieved in sidebands propagation, between the sidebands generator and the front end receiver mixer. The measured value at 1 000 GHz is 15 % with a 5 % contribution arising from the absorption cell. It has to be noticed that a proper adjustment of the polarising diplexers allows a single sideband operating mode.

The sidebands generator and detection diode systems have identical designs. They consist of gallium arsenide Schottky diodes mounted at the apex of a corner cube reflector.

The n^+ gallium arsenide substrate is covered with an insulating layer of SiO_2. An array of holes is etched in the insulating layer using lithographic techniques. A diode junction is established by making a point contact with a properly shaped Au-Ni wire on one site on the chip. The straight wire section located above the point contact determines the antenna length to which the radiation has to be coupled. The optical behavior of the antenna reflector assembly has been described by several authors [17, 18]. It has been demonstrated that the field pattern is governed ty two major parameters : the antenna length and the distance between the antenna and the corner apex.

Optimal performances are achieved when :

- the antenna length is a multiple of the working wavelength. 4 λ is often considered as a good compromise between antenna rigidity and relatively broadband capability ;
- the distance between the whisker and the corner equals 1.2 λ. The antenna pattern of the system is then concentrated in a single lobe centred on the reflector plane of symmetry. For any design departing noticeably from the previously described, the geometry of the antenna pattern exhibits side lobes. In such situations the sidebands generator radiates a fraction of the sidebands power outside of the experiment axis. This fraction of power is lost, contributing to a deterioration of the spectrometer sensitivity.

Any coupling loss at the diode detection input implicates a deterioration in the receiver noise temperature, as described by well-known classical formulae [19].

Resulting from previous observations, specifically designed mixer have been developed. The structure is very similar to the one previously described by Röser [20]. The semiconductor chip is directly glued on the central conductor of a section of rigid coaxial line. Combined to a double stub impedance matching technique at the mixer output, this solution leads to a reasonably lossless transmission through the coaxial path, between 2 and 18 GHz. These specific corner cube mounts provide a large improvement on the particular point of the radiofrequency bandwidth capability. This bandwidth rarely exceeds 2 or 3 GHz, in standard commercial products, with an approximate uppest limit at 6 GHz.

The Schottky diodes used in the actual instrument are 1T12 models, manufactured at the Virginia-Charlottesville University [19]. This diode family has been especially developed for submillimeter applications. The anode diameter is 0.1 μm. The antenna consists of a section of 25 μm diameter Au-Ni wire alloy (Fine wire of California). The wire end is sharpened by an electrolytic etching process.

For the sidebands generation, a Hewlett-Packard synthesizer (HP 83624 A) is connected to the diode *via* the coaxial port of the sidebands generator. The synthesizer provides frequencies in the range 2-18 GHz with a 1 Hz resolution. The maximum power is 20 dBm. In all common

experimental circumstances the power coupled to the sidebands generator is in the order of 15 dBm.

Starting from a laser emission in the range of some mW, the net sidebands radiated power scales between 5 and 20 μw. This power depends upon both the laser frequency and the radiofrequency values.

3.3 THE HETERODYNE RECEIVER. — A complete scheme of the receiver is given in figure 6. Two successive down conversions are performed through the system.

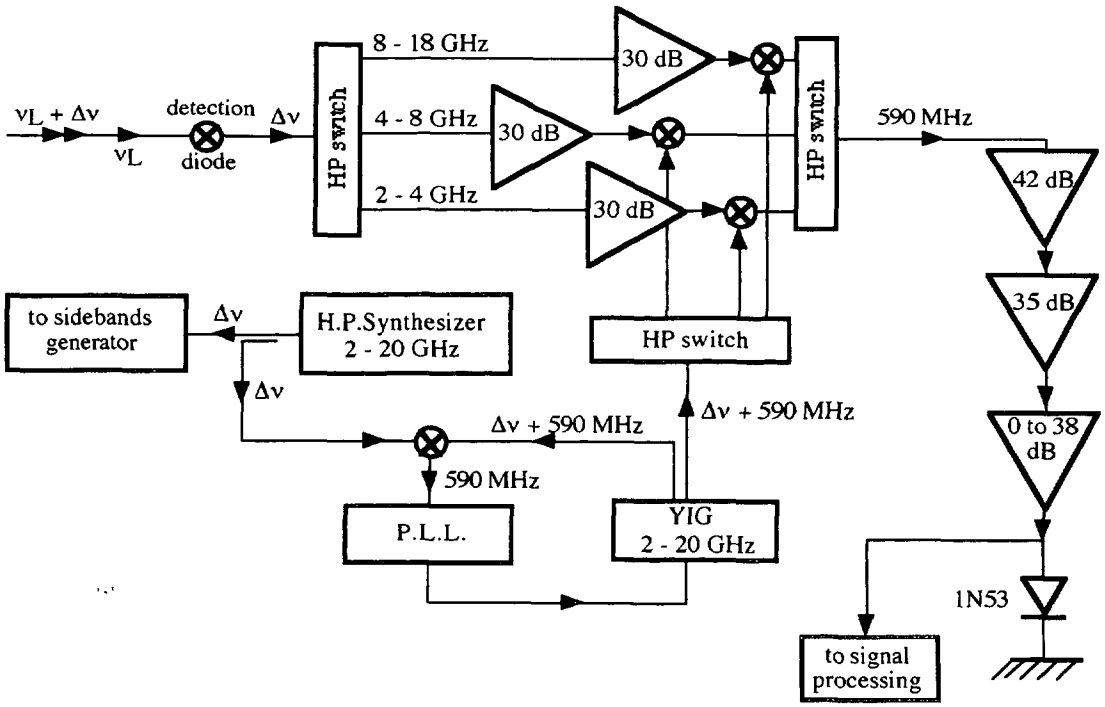


Fig. 6. — Details of the heterodyne receiver.

Designs are similar for the front end mixer and the sidebands generator previously described. At first, a mixing operation is performed between the laser frequency ν_L and the sidebands frequency $\nu_L \pm \Delta\nu$. A first intermediate frequency $\Delta\nu$ located in the range 2-18 GHz is obtained. The beat note frequency obviously follows the source frequency during the sweeping sequences.

The first intermediate frequency is amplified, in the appropriate selected bandwidth : 2-4 GHz, 4-8 Ghz or 8-18 Ghz. The amplifiers are low noise commercial devices models (AFT-4233, AFT-8433-Avantek and AMF7B 8018-60-Miteq). The typical noise figure is 3.5 dB for the two first amplifiers and 7 dB for the last one. The gain is of the order of 30 dB for every system.

After the first amplification stage, the beat note is down converted to a 590 MHz fixed frequency, using the following method.

A YIG 2-18 GHz oscillator (GO 3218-Giga-instruments) is phase locked, with a 590 MHz constant difference relative to the source synthesizer. The specific phase lock instrumentation

has been designed in the lab. The YIG emission is mixed with the amplified first intermediate frequency. A set of three low noise mixers is used for this function, respectively in the bandwidths 2-4 GHz, 4-8 GHz and 8-18 GHz (TFX 72, DBX 824-Avantek and M 0719-Miteq). So, the resulting beat note is a 590 MHz fixed frequency signal, with a fixed phase relation relative to the signal.

The remote bandwidth selection is performed using a set of 3 low losses SPDT switches (8767 K-Hewlett Packard).

The 590 MHz signal enters a cascade of 3 amplifiers :

- G = 42 dB BW = 500-700 MHz NF = 1.1 dB (AFS30-Miteq)
- G = 35 dB BW = 500-1 000 MHz NF = 3 dB (AM3A 0510-Miteq)
- G = 0-38 dB BW = 7 MHz centred at 590 MHz NF = 7.5 dB (Lab-made).

The third amplifier fixes the postdetection bandwidth of the heterodyne system.

At the output of the last amplification stage, the signal is detected using a 1N53 microwave diode. The resulting video signal is amplified through a low noise amplifier (mod. 113-PAR) with tunable gain and bandwidth. For spectroscopic uses in video mode, the bandwidth is (0.1 Hz-3 kHz) according to the 25 Hz sweeping frequency.

Tests and noise calibrations have been carried out on the electronic part of the receiver, in order to determine the sensitivity limits of the set-up. The noise figure has been measured using the Y factor method [17]. Following the general principle of this method a 50 Ω load is connected at the input of the first amplifier stage. This load is alternately left at ambient temperature, then immersed in a liquid nitrogen bath. The knowledge of the difference in the receiver output noise powers corresponding to the well defined temperatures of the input load allows the determination of the noise figure by straightforward calculations. The measured noise figure for the electronic part is 6 dB at 4 GHz corresponding to a noise temperature of 860 K. This value appears very close to theoretical limits estimated on the basis of data given by the manufacturers, concerning gain, losses or conversion losses of components. It is approximately constant on the 2-18 Ghz range.

The same Y factor method has been used for an estimation of the whole spectrometer noise figure. For measurements purposes, the sidebands generator is removed and alternately replaced by a mercury arc lamp and a 73 K cold load. The cold source is made of a piece of eccosorb (Emerson & Cumming) immersed in a liquid nitrogen bath. The arc mercury source is considered as a blackbody source at 2 300 K. In real experimental situations hot and cold sources are alternately switched at a 250 Hz frequency. The receiver response is processed by synchronous detection.

Under such conditions, the measured noise temperature is 12 000 K at 1 019 GHz, corresponding to a laser frequency emission of 1 015 GHz and a radiofrequency at 4 GHz. This noise temperature takes into account the conversion losses of the front end mixer and all propagation losses along the optical path.

A recent analysis of quadratic heterodyne receivers, based on an exact estimation of correlations between noise and signal components at the receiver input, yields to the expression of the minimum detectable spectroscopic signal [21]. This analysis exactly corresponds to the operating conditions of the actual system.

The minimum detectable change in source power ΔP_{min} is expressed by :

$$\Delta P_{min} = 2 \cdot \left(\frac{2\,\Delta f \,.\, \eta}{2P + \eta B} \right)^{\frac{1}{2}} \left(B\eta^2 + P^2 + 2B\eta P \right)^{\frac{1}{2}}$$

where : $\eta = FkT \,.\, F$ is the linear noise factor, k the Boltzmann constant and T the room temperature. ΔF is the system detection bandwidth (3 kHz). B is the predetection bandwidth (7 MHz). P is the source power (5-20 μW).

3.4 THE SIGNAL PROCESSING. — The data processing are performed using a Macintosh IIFX computer fitted with the Labview system from National Instruments. Two specific cards are employed in the actual version, models NB-MIO-16 and NB-DMA 2800. The synthesizer frequency is digitally driven. The computer generates a 200 points frequency list, with tunable limits and increment. The corresponding numeric commands are sent towards the synthesizer through an IEEE interface. The spectrometer can operate in the source modulation or in the video modes.

When used in the source modulation version, a sinusoidal modulation at $f = 100$ kHz is superimposed to each point of the frequency list of the synthesizer. After phase detection at $2f$ frequency, the signal has the shape of the second derivative of the line profile. The signal is handled by a 12 bits analog to digital converter. The computer performs at first a numerical averaging. The following operation consists of a frequency measurement of the line centre. Several options are available such as digital filtering, smoothing and base line compensation.

4. Spectroscopic example.

A typical spectroscopic record is shown at figure 7. The frequency center is close to 878 GHz corresponding to the CH_2CHF laser emission at 889 341.4 MHz, a radiofrequency at 10 970 MHz and minus sign in formula (1). The observed pattern corresponds to a K doubling observation in CH_3CF_3. Only the K3-component of the doublet can be seen in the figure. Complete spectroscopic results have been published elsewhere [22]. The half width line at half maximum is of the order of 1 MHz, close to the Doppler limit.

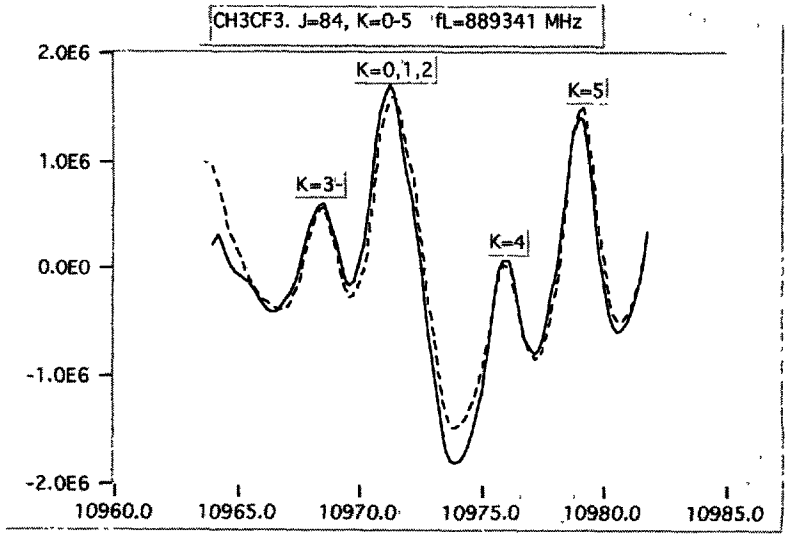


Fig. 7. — CH_3CF_3 spectrum at 878 GHz. Averaging on 3 scans. The solid line and the dashed line represent respectively the increasing and the decreasing recorded frequency spectrum.

5. Conclusion.

In the previous parts, we have described the far-infrared spectrometer built at Lille. The instrument operates under monochromatic, coherent and continuously tunable illumination. Some other systems, developed for similar applications have reached very high performance

levels. All known other systems retain a similar detection scheme, belonging to the so called direct detection principle.

The original feature of the instrument described in previous parts stands in its heterodyne receiver scheme. Such a detection system, although implying more complicated developments, exhibits some particular advantages.

As a first advantage, no optical filtering process is needed along the optical path. On the contrary, in direct detection systems, the primary laser power has to be lowered well below the useful sidebands power. Due to diffraction effects inherently attached to the long wavelength range, a very high rejection at ν and a very high transparency at $\nu \pm 10\ \%\ \nu$ constitute in facts almost contradictory constraints. As a consequence, direct detection system usually works in a compromise for which an amount of parasitic power has to be tolerated as well as some propagation losses into the filtering system. The former effect limits the detector sensitivity, the later raises the receiver noise temperature.

The experiment confirms the advantage of heterodyne systems relative to direct detection ones. It is particularly true at high resolution, as hardly established by theoretical considerations [23]. The lowest noise temperature for a broadband system has been reported by Röser *et al.* [24]. The instrument design departs noticeably from ours. The receiver was primarily developed for radioastronomic and atmospheric observations and, so, mainly for incoherent broadband illumination. The signal frequency analysis is performed by the receiver. This receiver is built around a dispersive acousto-optical system very similar to devices used in the most advanced millimeter radiotelescopes. Such systems integrate a part of cryogenic electronics and exhibit extremely low noise temperatures. On the other hand, their resolution is limited by the width of the elementary channel of the acousto-optical system, i.e. 1 MHz. Compared to typical Doppler widths, of the order of few megahertz on the spectral range of interest, such a resolution is well suited for astrophysical observations, but leads to severe limitations in spectroscopic applications.

Acknowledgements.

This work was supported by the Centre National de la Recherche Scientifique, the Institut National des Sciences de l'Univers and the Conseil Régional du Nord-Pas de Calais.

Authors thank Thomas Crowe of Virginia University-Charlottesville and H. P. Röser of Max Planck Institut-Bohn for their valuable help in design and realization of mixing devices. They thank P. Encrenaz and G. Beaudin of the Observatoire de Meudon for many helpful discussions on design of heterodyne receivers.

References

[1] Blake G. A., Laughlin K. B., Cohen R. C., Busarow K. L., Gwo D. H., Schmuttenmaer C. A., Steyert D. W., Saykally R. J., The Berkeley tunable far-infrared spectrometers, *Rev. Sci. Instrum.* **62** (1991) 1701-1716.

[2] Farhoomand J., Blake G. A., Frerking M. A., Pickett H. M., Generation of tunable laser sidebands in the far-infrared region, *J. Appl. Phys.* **57** (1985) 1763-1766.

[3] Verhoeve P., Zwart E., Versluis M., Drabbels M., Ter Meulen J. J., Leo Meerts W., A far-infrared sideband spectrometer in the frequency region 550-2700 GHz, *Rev. Sci. Instrum.* **61** (1990) 1612-1625.

[4] Piau G., Brown F. X., Dangoisse D., Glorieux P., Heterodyne detection of tunable FIR sidebands, *IEEE J. Quantum Electron.* **23** (1987) 1388-1391.

[5] Blumberg W. A. M., Fetterman H. R., Peck D. D., Tunable submillimeter sources applied to the excited state rotational spectroscopy and kinetics of CH_3F, *Appl. Phys. Lett.* **35** (1979) 582-585.

[6] Blumberg W. A. M., Peck D. D., Fetterman H. R., Sub-Doppler submillimeter spectroscopy using molecular beams, *Appl. Phys. Lett.* **39** (1981) 857-859.

[7] Martin D. H., Puplett E., Polarized interferometric spectrometry for the millimeter and submillimeter spectrum, *Infrared Phys.* **10** (1969) 105-109.

[8] Lambert D. K., Richards P. L., Martin-Puplett interferometer : an analysis, *Appl. Opt.* **17** (1978) 1595-1602.

[9] Nedvidek F. J., Kucerovsky Z., Brannen E., Far-infrared pump injection using an alumina waveguide, *Appl. Opt.* **26** (1987) 14-15.

[10] Roullard F. P., Bass M., Transverse mode control in high gain, millimeter bore, waveguide lasers, *IEEE J. Quantum Electron.* **13** (1977) 813-818.

[11] Harth A., Pump beam propagation in circular waveguide of optically pumped far-infrared lasers, *Int. J. Infrared Millimeter Waves* **12** (1991) 221-237.

[12] Douglas N. G., Millimeter and submillimeter wavelength lasers (Springer-Verlag, 1989).

[13] Costley A. E., Hursey K. H., Neill G. F., Ward J. M., Free-standing fine-wire grids : Their manufacture, performance, and use at millimeter and submillimeter wavelengths, *J. Opt. Soc. Am.* **67** (1977) 979-981.

[14] Erickson N. R., Off-axis mirrors made using a conventional milling machine, *Appl. Opt.* **18** (1979) 956-957.

[15] Boucher D., Burie J., Bocquet R., Chen W., Quasi-optical mirors made by a conventional milling machine, *Int. J. Infrared Millimeter Waves* **13** (1992) 1395-1402.

[16] Shapiro J. B., Bloemhof E. E., Fabrication of wire-grid polarizers and dependance of submillimeter wave optical performance on pitch uniformity, *Int. J. Infrared Millimeter Waves* **11** (1990) 973-980.

[17] Fetterman H. R., Tannenwald P. E., Clifton B. J., Parker C. D., Fitzgerald W. D., Erickson N. R., FIR heterodyne radiometric measurements with quasi optical Schottky diode mixers, *Appl. Phys. Lett.* **33** (1978) 151-154.

[18] Grossman E. N., The coupling of submillimeter corner-cube antennas to Gaussian beams, *Infrared Phys.* **29** (1989) 875-885.

[19] Crowe T. W., Wood P. A. D., Peatman W. C. B., Rizzi B. J., « GaAs Schottky Diodes for Mixing Applications Beyond 1 THz », 16th Int. Conf. Infrared Millimeter Waves, Lausanne Switzerland (26-30 August 1991) pp. 468-469.

[20] Röser H. P., Heterodyne spectroscopy in the far-infrared, *Europhys. News* **21** (1990) 195-200.

[21] Boucher D., Bocquet R., Chen W., Burie J., Ultimate sensitivity of heterodyne spectometers, *Int J. Infrared Millimeter Waves* **14** (1993) 1889-1903.

[22] To be published in the *J. Mol. Spectrosc.*

[23] Harris A. I., « Coherent and incoherent detection at submillimeter and far-infrared wavelengths », Coherent detection at millimeter wavelengths and their application, Les Houches France March 1990, P. Encrenaz, C. Laurent, S. Gulkis, E. Kollberg and G. Winnewisser, Eds. (Nova Science Publishers, 1991) pp. 7-34.

[24] Röser H. P., Wattenbach R., Durwen E. J., Schultz G. V., A high resolution heterodyne spectrometer from 100 μm to 1 000 μm and the detection of CO ($J = 7 - 6$), CO ($J = 6 - 5$) and ^{13}CO ($J = 3 - 2$), *Astron Astrophys.* **165** (1986) 287-289.